Analytica Chimica Acta 1069 (2019) 36–46

Contents lists available at ScienceDirect

Analytica Chimica Acta

journal homepage: www.elsevier.com/locate/aca

Scanning electrochemical microscopy with conducting polymer probes: Validation and applications

Marie A. Claudio-Cintrón, Joaquín Rodríguez-López*

Department of Chemistry, University of Illinois at Urbana-Champaign, 600 South Mathews Avenue, Urbana, IL, 61801, United States

HIGHLIGHTS

- Stable modified probes for SECM were fabricated using conducting polymers as electrode material.
- Response and spatial resolution of modified probes was comparable with conventional Pt probes.
- SECM imaging was successfully performed using both a conventional mediator (Fc) and an unusual one (DMcT).

ARTICLE INFO

Article history:
Received 31 December 2018
Received in revised form
5 April 2019
Accepted 9 April 2019
Available online 15 April 2019

Keywords:
Conducting polymers
Scanning electrochemical microscopy
Modified electrode probe

ABSTRACT

Scanning electrochemical microscopy (SECM) allows spatially and temporally resolved measurements of a broad range of reactive surfaces and specimens, typically using electrochemically active metal probes. While conducting polymers (CPs) present several analytical properties of interest due to their chemical versatility, potentially enabling the measurement of ionic fluxes as well as redox processes, they have not been widely used as probe materials for SECM. CPs can be modified and fine-tuned to improve experimental parameters and they can be easily prepared by electrodeposition. In this paper, we show a new type of CP probe for SECM that retains the spatial resolution of conventional metal probes and introduces the possibility to exploit a wide range of ionic and redox systems. Poly-3,4-ethylenedioxythiophene (PEDOT) was electrochemically deposited on flat and recessed Pt microdisks to generate CP SECM probes. To demonstrate their usefulness, an insulating substrate with conducting features was imaged. Well-defined SECM feedback images were observed for both the CP well-probe and the Pt probe, proving the efficiency of the new electrode to image redox reactions. Additionally, an organosulfur compound was used as mediator taking advantage of the electrocatalytic effect PEDOT has on the molecule's kinetics. Finally, these probes were also used in a mediator-less fashion, taking advantage of the ion flux required to electrochemically oxidize the PEDOT deposit. We investigated the impact of anion size and concentration on current-distance relationships for SECM probe positioning. CP probes pose exciting prospects for the imaging and measurement of combined redox and ionic processes in energy materials.

1. Introduction

Scanning electrochemical microscopy (SECM) is a scanned probe technique capable of measuring redox and ionic reactivity on a variety of substrates, including interphases of battery materials [1,2], conducting surfaces with heterogeneous reactivity [3,4], and studying a variety of systems from metal corrosion to living cells [5,6]. In the feedback mode of SECM, the probe consists of an electrode that enables the imaging of surface reactivity by detecting changes in current as a redox mediator is cycled in the gap between probe and substrate. This current responds to changes in its local environment thus allowing the measurement of differential responses to topographic and reactive features [7]. Because the probe electrochemistry is customizable, several modes and hybrid techniques have been developed over the years that allow for determination of a broad variety of reactions, including electron transfer [8], ion transfer [9], adsorbed intermediate quantification [10,11], photoelectrochemical response [12,13], electrocatalysis [14], amongst many others [15].

An active direction in SECM studies is the development of new types of probes for both amperometric and potentiometric measurements [16–19]. There is currently a wide variety of probes

* Corresponding author.
E-mail address: joaquinr@illinois.edu (J. Rodríguez-López).

https://doi.org/10.1016/j.aca.2019.04.022
0003-2670/

including ultra-micro electrodes (UMEs), in which a conducting wire is sealed in a glass capillary and then exposed to reveal a flat disk ranging from 25 μm in radius to the nanoscale [20–22]. Probes for hybrid techniques such as SECM-AFM (atomic force microscopy) have allowed the determination of topographical and electrochemical information by recording the interaction force with the AFM probe and the current with the electrode [23–28]. Furthermore, there is an ever-increasing interest in exploring the versatility of SECM probes for chemical imaging. For example, the interest in measuring ion fluxes in biological systems has led to the development of probes based on ion transfer across the interface between two immiscible electrolyte solutions (ITIES) [29–32]. Similarly, our group has introduced probes based on Hg for imaging alkali ions in battery solvent environments for operating energy storage interfaces. In addition to the use of Hg probes, impedance modes of SECM and Scanning Ion Conductance Microscopy (SICM) for imaging ion fluxes have proved the potential of mediator-free systems [33–37].

An attractive direction in SECM probe development involves modifying the electrode by adding an electroactive polymer layer, thus granting the electrode additional properties like selectivity for anions, enhanced catalytic activity, or increased probe stability [38,39]. Modified electrodes have also been employed as alternatives to reduce the surface fouling observed with the measurement of certain analytes, often due to unwanted side reactions or irreversible adsorption [40,41]. It would be desirable to incorporate as many of these sought-after properties into a single probe. Here, we explore the properties of one such probe that takes advantage of the unique attributes of conducting polymers (CPs) for the measurement of redox and ionic processes, while also avoiding electrode fouling.

CPs consist of repeating units of conjugated organic molecules that are easily prepared via electrochemical methods [42]. Furthermore, their backbone can be modified to improve on their electronic, physical, and optical qualities [43]. Thus, these materials have found many applications in fields such as electrocatalysis, electronics, energy, coatings, electromagnetic shielding, and sensors [44]. The attractiveness of CPs as materials for SECM probes stems from their combined electronic, redox and ionic properties. CPs display high chemical stability, and conductivity [45,46]. They can mediate reactions while in their conductive state, making them viable as electrode materials for SECM (Fig. 1A) in the feedback mode. As long as the standard reduction potential (E^0) of the redox mediator is within the conductivity window of the CP, it should be sufficient to perform redox chemistry on the mediator [41,47,48]. Conductivity in CPs is based on doping, where electrons are removed through oxidation (p-doping) or added through reduction (n-doping). These processes efficiently delocalize charge along the backbone. Upon charging and discharging the electrolyte ions diffuse into the polymer matrix, effectively neutralizing the charges formed along the backbone of the doped polymer (Fig. 1B) [39,42,44,49,50].

Because of these operation modes, we hypothesized that CP-modified SECM probes would provide a versatile platform for measuring redox and ionic processes. In their conductive state, CPs will mediate the redox reaction of a species in solution allowing for redox imaging of a substrate. Likewise, affecting the flux of ions to the material during the doping reaction would result in currents reflecting changes in local ionic activity. The recent work from Venugopal et al. [51] studying the insertion of cations on a CP in an SECM configuration, and studies on the process of ionic transport within CP films by Wang et al. give us a theoretical framework in which to base our hypothesis [52–54]. Combining these properties would allow for measurements of systems with new types of mediators and to expand on the potential of conducting polymers as an analytical tool.

Conducting polymer films have already been employed in modified electrodes where a thin film of the polymer is deposited onto a surface. These modified electrodes are especially useful in enhancing or improving the selectivity of the probe towards certain analytes or electrochemical reactions [41,55–58]. Though SECM has been employed for many applications involving CPs [26,59–61], and CPs have been used to modify UMEs and perform analytical measurements [51,62], these have yet to be employed in SECM probes for redox and anion measurement. In the following sections we describe a method through which poly-3,4-ethylenedioxythiophene, commonly known as PEDOT [63], was successfully deposited into a recessed cavity etched into an UME (Fig. 1). We then used this modified well-electrode as an SECM probe to image features on a both insulating and conducting substrate. Later, we show that these CP probes provide an avenue to expand mediator choice for SECM by using an organosulfur compound as a mediator, which typically cannot be done on noble metal electrodes due to slow kinetics and fouling of the electrode [64]. To demonstrate versatility of this approach, we used cyclic voltammetry (CV) and various counter anions to study the possibility of utilizing this probe for the study of ion fluxes [33,34].

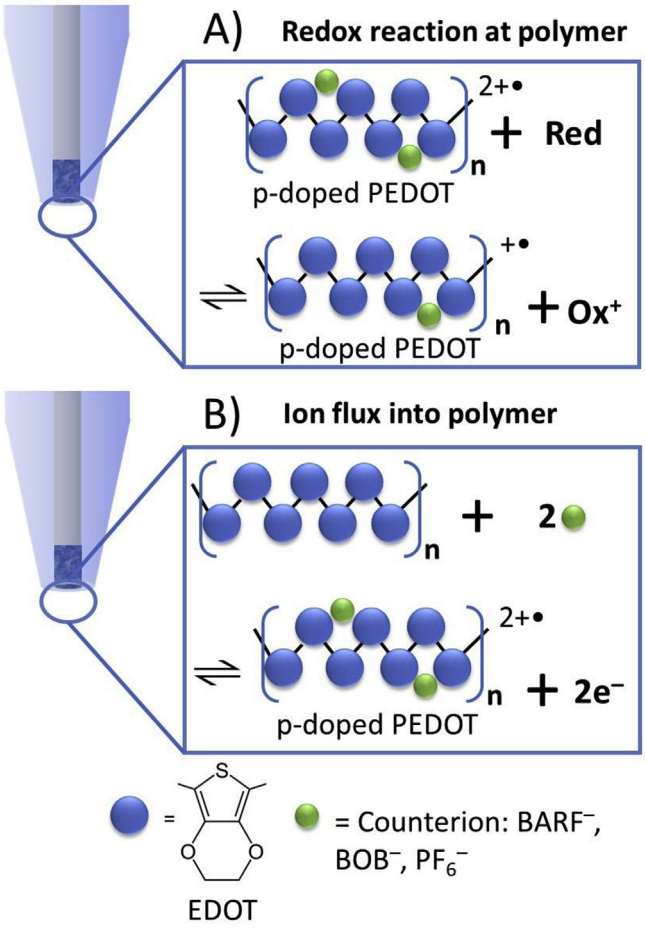

Fig. 1. Mechanisms for detecting charge transfer reactions at CP-modified SECM probes. A) Redox reaction mediated by p-doped PEDOT. B) Influx of counterions upon doping.

2. Materials and methods

2.1. Reagents

Calcium chloride ($CaCl_2$, Sigma, 99+%), 3,4-

ethylenedioxythiophene (EDOT, $C_6H_6O_2S$, Aldrich, 97%), ferrocene (Fc, Aldrich, 98%), lithium bis(oxalato)borate (LiBOB, Aldrich), lithium tetrakis(3,5-bis(trifluoromethyl)phenyl)borate (LiBARF, Boulder-Scientific), tetrabutylammonium hexafluorophospate ($TBAPF_6$, Sigma-Aldrich, 99+%), tetrabutylammonium tetrafluoroborate ($TBABF_4$, Sigma-Aldrich, 99+%), 1,3,4-thiadiazole-2,5-dithiol dipotassium salt ($DMcTK_2$, Sigma Aldrich, 98%), hydrochloric acid (HCl, Macron), acetonitrile (AN, Fisher Chemical, 99+%), and N,N-dimethylformamide (DMF, Sigma-Aldrich, 99.8%) were purchased from commercial sources and used as received. Millipore deionized water with resistance ≥18 MΩ was used.

2.2. Probe fabrication

Pt disc UMEs were fabricated by sealing a Pt wire of radius (a_1) 12.5 or 25 μm inside a borosilicate glass capillary by using a Narashige PE-2 glass puller. Another UME of radius 3.5 μm was fabricated by electrochemically etching a 12.5 μm Pt wire by applying 2.70 V to the wire while submerged in a solution composed of 30 v. % sat. $CaCl_2$ + 10 v. % HCl in H_2O, using a carbon rod as a counter electrode [65,66]. Afterwards, the wire was sealed in a glass capillary as detailed previously. The electrodes were then sharpened using a beveller to reduce the area of glass around the wire and decrease the total probe radius (a_2). After sharpening, the probes were polished using a felt polishing pad covered in a 1 μm alumina (Al_2O_3) slurry (Fig. 2A).

Following the determination of the Rg (a_2/a_1) by optical methods, the electrodes were etched/recessed using the same etching solution specified previously and applying a 2.70 V AC waveform at 60 Hz with a variac for 40s (Fig. 2B). This resulted in a cavity of about 12.5 μm, or the same radius as the electrode probe. The probes were sonicated during etching to avoid retention of bubbles in the cavity as specified elsewhere [33].

For the deposition of the CP, a 10 mM EDOT solution with 0.1 M $TBAPF_6$ as electrolyte in AN was used. Each probe was sonicated briefly in the solution prior to deposition to guarantee contact with the recessed Pt disk. The polymer (PEDOT) was electrodeposited potentiodynamically for at least 15 cycles in the potential window between −0.1 and 1.35 V vs Ag/AgCl (Fig. S1A). After deposition, the excess polymer that covered the surface above the glass was carefully removed with a lint-free wipe wetted with AN, leaving polymer only within the recessed electrode cavity (Fig. 2C) [33]. These probes that have been etched back are referred to as "well-probes." For the deposition of a film on a Pt disk, only 1 cycle was performed and was not sonicated or treated after deposition (Fig. S1B). This probe is referred to as "film-modified."

2.3. Electrochemical tests

With exception of the probe fabrication, deposition and testing of the polymer, all experiments including SECM and CV-SECM were conducted in a MBRAUN UNIlab glovebox operating under ultra-high purity argon. Bipotentiostat CHI 920D was used for all measurements inside the glovebox and CHI 760 was used for probe fabrication (both from CH Instruments). A Pt wire served as a counter electrode and a silver wire as a quasi-reference. Where appropriate, CVs were referenced against Ag/AgCl using the redox couple ferrocene/ferrocenium (Fc/Fc^+) as an internal standard added at the end or the beginning of the experiment.

2.4. Scanning electrochemical microscopy

Experiments were performed using a standard SECM Teflon cell [15]. The substrate was leveled by performing a 700 μm line scan along the *x* and *y* axes sequentially and adjusting the tilt of the stage until the difference in current from one side to the other was less than 1%.

Imaging using the conducting polymer probe was performed using a PEDOT well-probe, a PEDOT film-modified electrode, and a Pt disk UME. The substrate consisted of an electrode array, where 15 μm radius Pt circles were exposed through a patterned SU-8 photoresist spin-coated on a silicon dioxide (SiO_2) wafer. The Pt circles were connected to leads that could be used to activate the substrate (Figs. S4–5). The approach curves for each electrode were fitted to theoretical curves for negative feedback as described elsewhere [33]. The distance for the approach curves are expressed

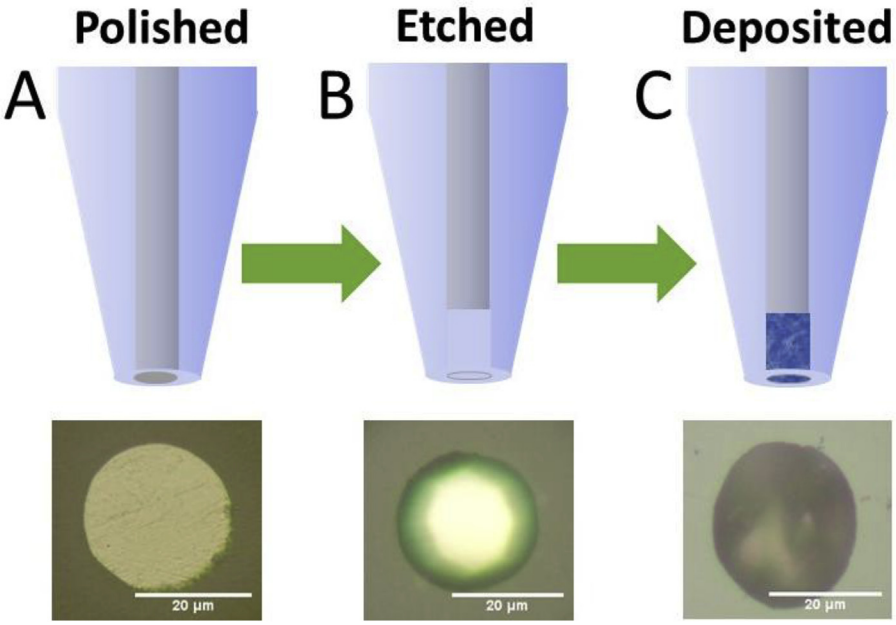

Fig. 2. Fabrication process of a polymer well-probe. Optical images (50x) of the top of the probe after each step. A) Electrode polished and sharpened. B) After electrochemical etching with 30 v.% sat. $CaCl_2$ + 10 v.% HCl in H_2O. C) After deposition of PEDOT by cycling in a monomeric solution of EDOT and wiping surface with lint-free wipe.

in terms of L where $L = d/a_1$, d is the absolute distance in μm [5]. A region of interest was found after leveling the surface and imaged using the substrate without bias and later while biasing it in competition mode at the same potential the tip was applying (1.0 V vs Ag QRE). Imaging with the PEDOT well-probe was compared with two others to confirm viability of the probe: one consisting of a bare Pt disk and a modified electrode with a thin film of PEDOT covering a Pt disk electrode. Probes used in these experiments were 12.5 μm in radius. The images obtained with the bare Pt disk UME were used as control. The size of the probes was appropriate to resolve the features on the substrate. The current obtained was then normalized by the limiting current at infinite distance.

The substrate used for CV-SECM using $DMcTK_2$ as mediator consisted of 50 μm-deep ridges on polydimethylsiloxane (PDMS) (Fig. S6). The surface was approached and imaged with a Pt UME and a PEDOT well-probe using a 10 mM, 0.1 M $TBAPF_6$ solution in DMF. The cell was then rinsed with DMF and the solution was changed to a 2 mM DMcT +0.1 M $TBAPF_6$ in DMF and the same procedure was repeated.

Ion-flux experiments used the stepper and piezo motors of the SECM to approach to an insulating surface (glass). A 10 mM, 0.1 M $TBAPF_6$ solution in DMF was used to locate the substrate before rinsing the cell and changing the solution to one containing one of the anions under study.

3. Results and discussion

3.1. Characterization of probes

PEDOT was deposited at the electrode surface by potentiodynamic cycling of the probe (Fig. S1). The thickness of the PEDOT inside the well-probes was the same as the depth of the cavity since the film was trimmed to be at the same level as the glass after deposition. Scanning electron microscopy (SEM) images (Figs. S3A and S3B) confirmed the presence of the film and revealed the morphology of the film inside the cavity before and after an experiment. Cycling the probe in clean electrolyte solution after cleaning the excess polymer confirmed electrochemical connectivity to the electrode surface and represented a typical voltammogram for a PEDOT film (Fig. S2).

The film deposited on the Pt disk UME revealed the presence of a ring, indicating a thicker deposit of PEDOT when compared to the center of the UME (Fig. 4a, inset). This ring often forms around the electrode surface due to the higher flux of electroactive species, in this case, EDOT oligomers, to the edges of the electrode [67]. SEM images of the well-probe revealed heterogeneity at the surface of the electrode (Fig. S3), as the film was not level in its entirety with the glass. However, this did not affect our measurements, or the performance of the probe, as will be shown in later experiments. As seen in Fig. S3B, the main morphological features, including the presence of a cavity, and irregular edges and deposits were observed before and after imaging. We did not observe changes either when the probe was exposed to air for 48 hrs, with exception of the layer losing contact with the edges of the cavity as the solvent evaporated. The probe can be used after several days of being fabricated, as long as it is cycled in electrolyte before use. However, for these experiments we used a freshly made probe before each experiment.

3.2. Feedback measurements using redox processes

The mediator used for this experiment was the Fc/Fc^+ redox couple, a well-known and reversible mediator for SECM [68]. The voltammetry for the oxidation of Fc was observed over the background signal for charging and discharging of the polymer film for

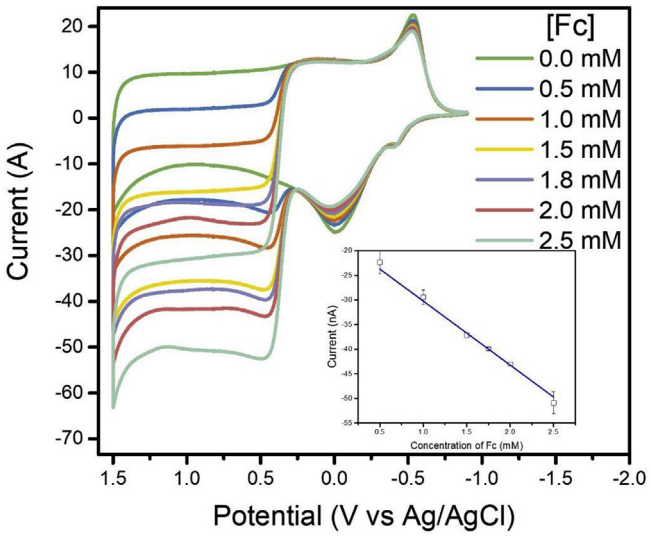

Fig. 3. Redox mediation at CP-SECM probes. Increasing concentration of Fc in a 0.1 M $TBAPF_6$ solution in AN at a PEDOT well-probe at 50 mV/s. Insert) Steady state current plotted vs concentration. Error bars were obtained from three replicates.

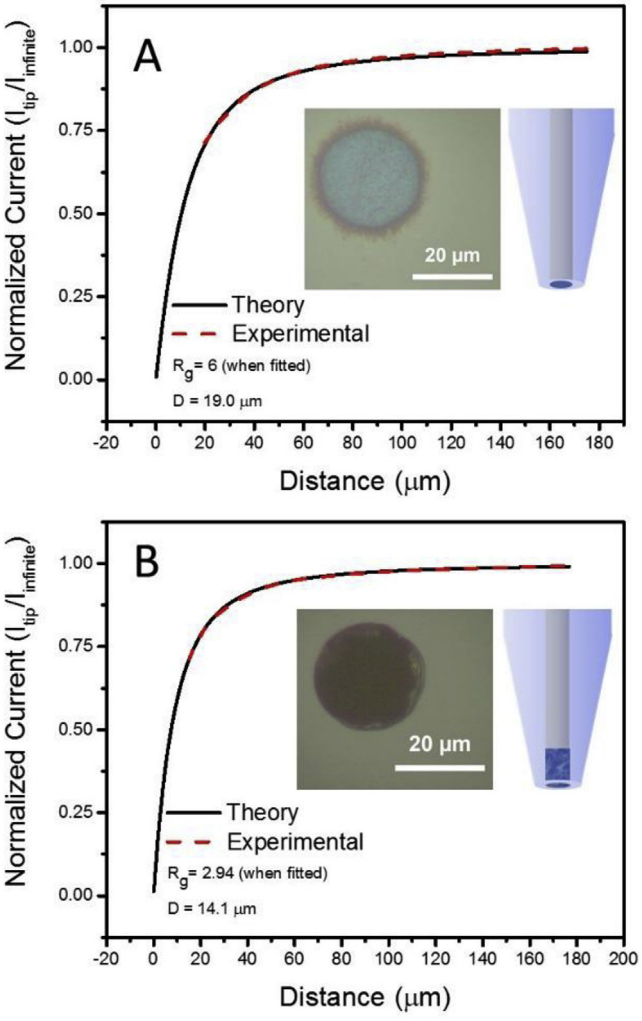

Fig. 4. CP SECM probe approach curves to glass using a redox mediator. Comparison between A) electrode modified with a thin film of PEDOT and B) a CP well-probe. Edge effects can be observed for the first case, whereas excess deposited polymer can be easily removed from the well-probe. Performed at 10 mM Fc + 0.1 M $TBAPF_6$ in DMF.

both the film-modified and the well electrodes (Fig. 3). To study the relationship between the concentration of mediator and steady state current, Fc was spiked into a 0.1 M $TBAPF_6$ solution while maintaining a constant concentration of electrolyte. A linear relationship was obtained between the concentration of Fc and steady state current of the PEDOT well-probe (Fig. 3, insert). Assuming that the electrode response is characterized by the limiting current at a disk microelectrode with radius *a*, for a process displaying one electron (n = 1) as is the case for ferrocene, with a diffusion coefficient of 2.3×10^{-9} m^2/s in MeCN, and with F = 96,485 C/mol, the

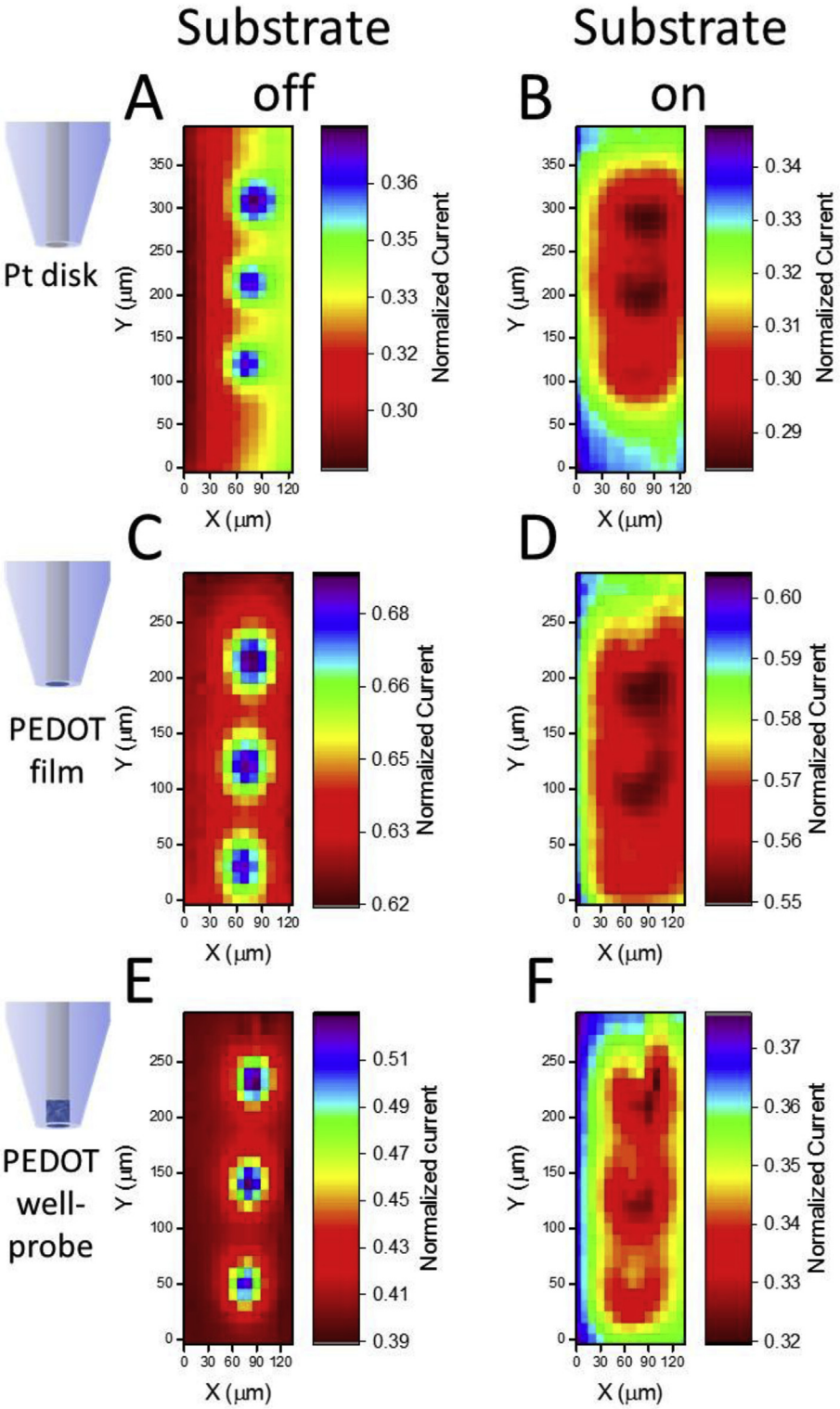

Fig. 5. Feedback and Redox competition mode imaging comparison between Pt and CP-modified SECM probes. 10 mM Fc + 0.1 M $TBAPF_6$ in DMF. SECM image of a substrate in competition mode using three types of r = 12.5 μm probes with the substrate unbiased (A, C and E) and with the substrate biased to compete with the probe (1.0 V vs Ag QRE) (B, D and F). A, B) Pt UME C, D) PEDOT film modified UME E, F) PEDOT well-probe UME.

slope (m) of a current vs. concentration plot such as that shown in Fig. 3 can be calculated as $m = 4nFaD$, leading to $m = 1.1 \times 10^{-8}$ A/mM. We experimentally found a slope of 1.3×10^{-8} A/mM, which is in agreement with the theoretically predicted value. A slightly larger value may be explained by the presence of a larger electroactive area, which could be caused either by a slight protrusion of PEDOT or polymer present beyond the boundaries set by the cavity. Although Fig. S3 shows a complex morphology of the PEDOT deposit, the characteristic times used for voltammetry and for the SECM approach curves allow a growth of the diffusion layer that exceeds the size of the non-uniformities, thus leading to a limiting current that approaches that of a flat microdisk. This suggested that the signal for the mediator should decrease as the probe is approached to an insulating surface (i.e. SECM negative feedback) due to inhibited diffusion of mediator to the tip. Thus, this allows the use of the redox couple as mediator for imaging when using a PEDOT-modified probe.

The CP probes were subsequently brought close to an insulating glass surface. Fitting of the obtained approach curves was in agreement with negative feedback theory (Fig. 4 and Table S1) [33]. Although the ring effect increases the effective surface area of the PEDOT-film-modified electrode and impacts the geometry of the electrode (Fig. 4A), we did not observe an effect on the ability to use reported expressions for approach curves. Both the film and the well-probe reached within 2L (25 μm) from the surface, allowing for imaging of surface features. We believe the disc-well is a more suitable probe since in the event of crashing with the surface, it would experience a minimal damage since its polymer filling is level with the insulating glass. In contrast, the film-modified electrode raised polymer layer would be deformed or scratched after crashing, negatively affecting its performance.

3.3. Imaging a conducting and insulating substrate

A substrate with 30 μm diameter Pt disks was imaged with a Pt disk UME, a PEDOT film-modified probe and a PEDOT well-probe. All probes had a $Rg < 5$ and a 12.5 μm radius. Fc/Fc^+ was used again as a mediator for this experiment. The region of interest was first imaged while the substrate was off (e.g. at open circuit potential). Under these conditions, any observed differences in current over the spots are due to lateral charge diffusion at the Pt surface, causing the current to be effectively larger than at completely insulating regions (Fig. 5, left). The difference in geometry caused by the ring of polymer in the film-modified disk caused a decrease in the imaging resolution, making the features appear larger than they are (Fig. 5c). This was not caused by differences in imaging distance. Redox competition imaging also evidenced image variations. Here, the substrate was biased to an oxidizing potential for Fc, while the same reaction is carried out at the tip. This is shown in the "on" version of the image (Fig. 5, right). Once again, we can more clearly distinguish the three spots with the well-probe UME than with the film-modified probe. From this experiment, we concluded that the well-probe resulted in a suitable tip for imaging, and that imaging resolution was not greatly affected by the heterogeneity observed with the SEM. These probes performed similarly to the Pt UME. The film-modified probe did not perform as well as the well-probe, which can be attributed to several factors such as the thicker polymer edge ring and the overall amount of polymer. These affect the probe geometry and the film stability since there is significantly less amount of polymer in the film than in the well.

3.4. Utilization of DMcT as a mediator for SECM

Previous work by the Abruña group studied organosulfur compounds as viable molecules for energy storage in lithium-ion batteries. These molecules show slow reaction kinetics on noble metals such as Pt but their reactions are catalyzed on conducting polymers. Particularly with PEDOT, these demonstrate faster kinetics (Fig. S17) [64]. Preliminary experiments with DMcT (Fig. S18) show a progressive fouling of the Pt surface that leads to distorted SECM approach curves. We speculate that this occurs due to the deposition of sulfur-containing species on Pt which block electron transfer. These complications are remedied when using a CP well-probe, thus demonstrating their potential for systems that interfere with metallic electrodes [69,70]. We tested the viability of using one such organosulfur compound, 1,3,4-thiadiazole-2,5-dithiol in its potassium salt form ($DMcTK_2$), as a mediator to image topographical features on a substrate. The substrate consisted of 50 μm-wide and 50 μm-deep ridges patterned on PDMS which were 150 μm apart. To fully demonstrate the resistance to fouling, we used an overpotential of 20 mV after the second oxidation of DMcT. A 200 μm by 200 μm area of interest, where a ridge can easily be observed, was imaged using the second oxidation potential. To compare with a trusted mediator, Fc was used again in the same concentration as before (10 mM, 0.1 M $TBAPF_6$ solution in DMF) and the level of contrast obtained was the same for both as can be seen in Fig. 6. Differences in current levels can be attributed to different absolute heights from the surface. For each mediator, a separate approach was done where imaging distance from the surface was 0.9L (11.25 μm) for DMcT and 0.75L (9.38 μm) for Fc, where both distances created distinct levels of contrast. Approach curves and

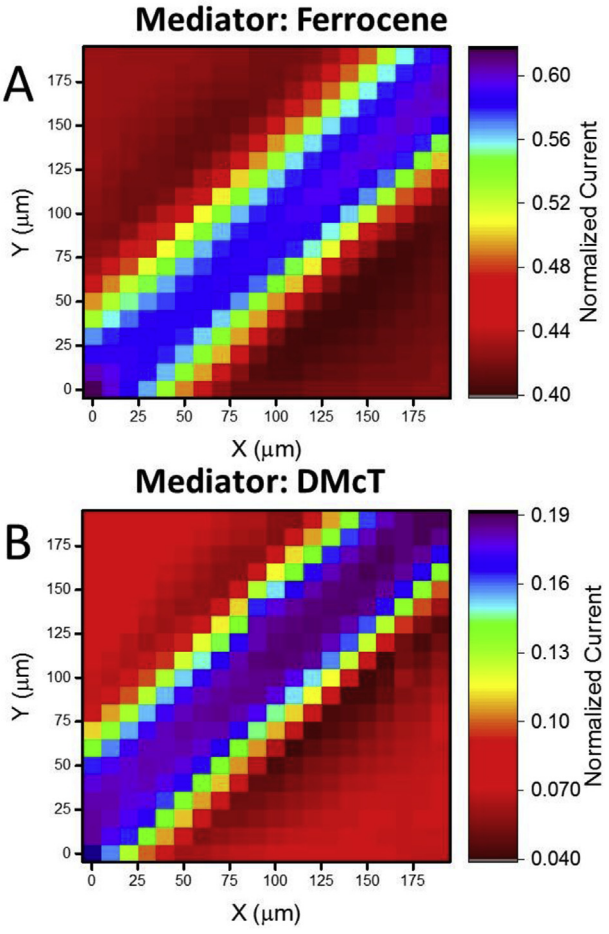

Fig. 6. SECM imaging in feedback mode of a ridge imaged with A) 10 mM Fc + 0.1 M $TBAPF_6$ in DMF and B) 2 mM DMcT +0.1 M $TBAPF_6$ in DMF.

fitting parameters can be found in Fig. S16 and Table S2. Despite different distances from the surface, both are acceptable for imaging with good contrast. The feature imaged had the same dimensions and in both cases the images showed excellent level of contrast. This experiment proved the ability of the probe to use an organosulfur compound redox system as a mediator for SECM during imaging. We have proven the usefulness of the PEDOT well-probe for redox imaging in SECM. We now turn to exploring the prospects of using it for ionic imaging.

3.5. Ionic flux measurements using CV-SECM

To test our hypothesis that counterions from the electrolyte could be used for differentiating ionic fluxes when coupled to charge transfer reactions (Fig. 1B), different anions of varying size were tested with a PEDOT well-probe. The strategy used here consists of measuring the current at the CP-SECM probe when starved of charge-compensating ions. Fig. 7 shows a preliminary experiment where the difference in capacitance (i.e. current normalized by scan rate) of a PEDOT well-probe was measured in the presence of different sized anions in solution. Furthermore, the probe response is also sensitive to the concentration of electrolyte (Fig. S19). The flux of electrolyte at different scan rates also affects the charge neutrality along the film, in turn affecting the capacitance [51]. These two results suggest that limiting the rate at which ions are inserted into the CP will lead to a differentiated probe response. This is precisely what one encounters in the negative feedback mode of SECM, where diffusion of ions to the probe is blocked as it is approached to a surface.

Figs. 8 and 9 show the probe response as it is approached to an insulating surface. The experiment took advantage of the technique CV-PAC described previously by Barton et al. [33] in which a cyclic voltammogram is taken at various steps as the probe is moved toward a surface, and then a PAC is constructed with the resulting current at some chosen potential, in this case the current at 1.1 V. For a control, the insulating surface was first approached using a conventional probe approach curve (PAC) using a redox mediator. Once the surface was located, a point within 2L ($L = d/a$ where d is the distance and a is the probe radius) from it was denominated as 0 μm. This was the point where the probe was closest to the surface. Approach curves were obtained over a range of 14 L [33]. After determining the distance where this condition was true for each electrode size, the probe was moved toward the surface at differently sized steps until it reached 0 μm.

At each step or distance away from the surface, the probe took cyclic voltammograms at different scan rates, to test how this parameter affects the charging of the film with the different anion sizes and the role of limited diffusion caused by the proximity to the surface. For smaller anions (PF_6^-), the change in current was less when compared with the larger anions (Fig. S13). This was expected given the small molecular size and faster diffusion coefficient compared with larger anions, giving them more ease to diffuse into the polymer matrix while charging, regardless of the limited space in the probe tip as it got closer to the surface. As expected, the largest anion, $BARF^-$, showed more contrast in the anodic charging current, decreasing as the probe got closer to the surface, and showed the same trend if the probe was moved backward starting from the surface to the point of D = 14 L (Fig. 8). This trend

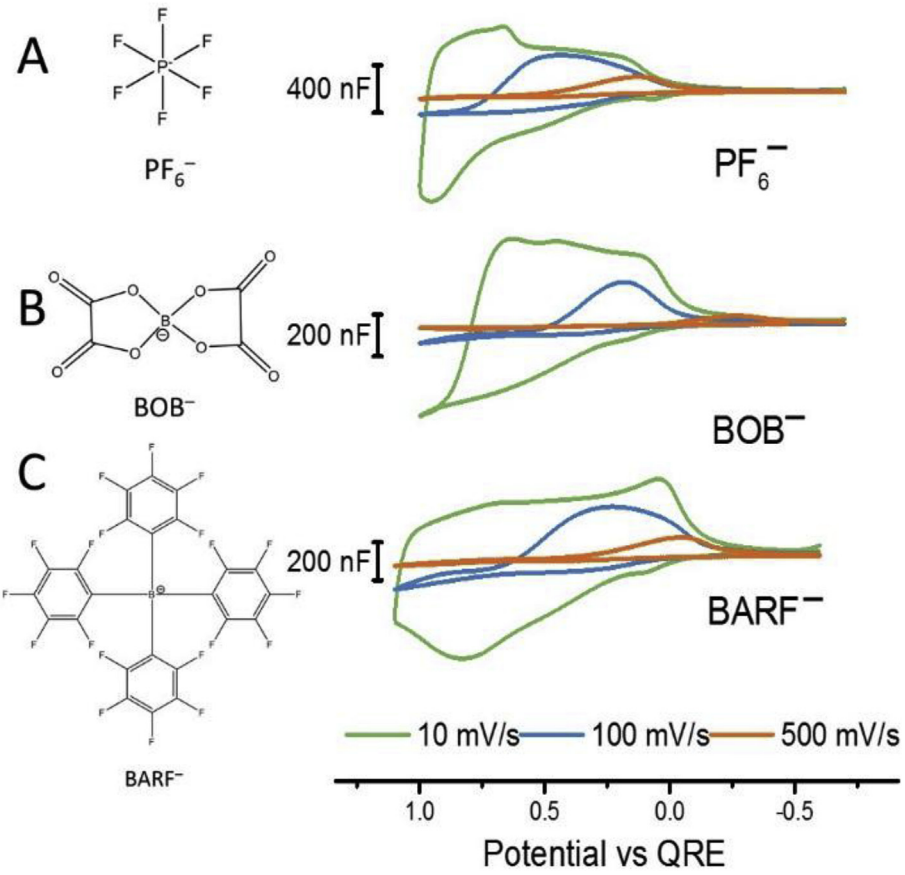

Fig. 7. Cyclic voltammograms measured against Ag QRE showing the capacitance of the PEDOT well-probe UME in the presence of different anions all in 1 mM in DMF at different scan rates. A) tetrakis(3,5-bis(trifluoromethyl)phenyl) borate ($BARF^-$) B) bis(oxalato) borate (BOB^-) C) hexafluorophospate (PF_6^-).

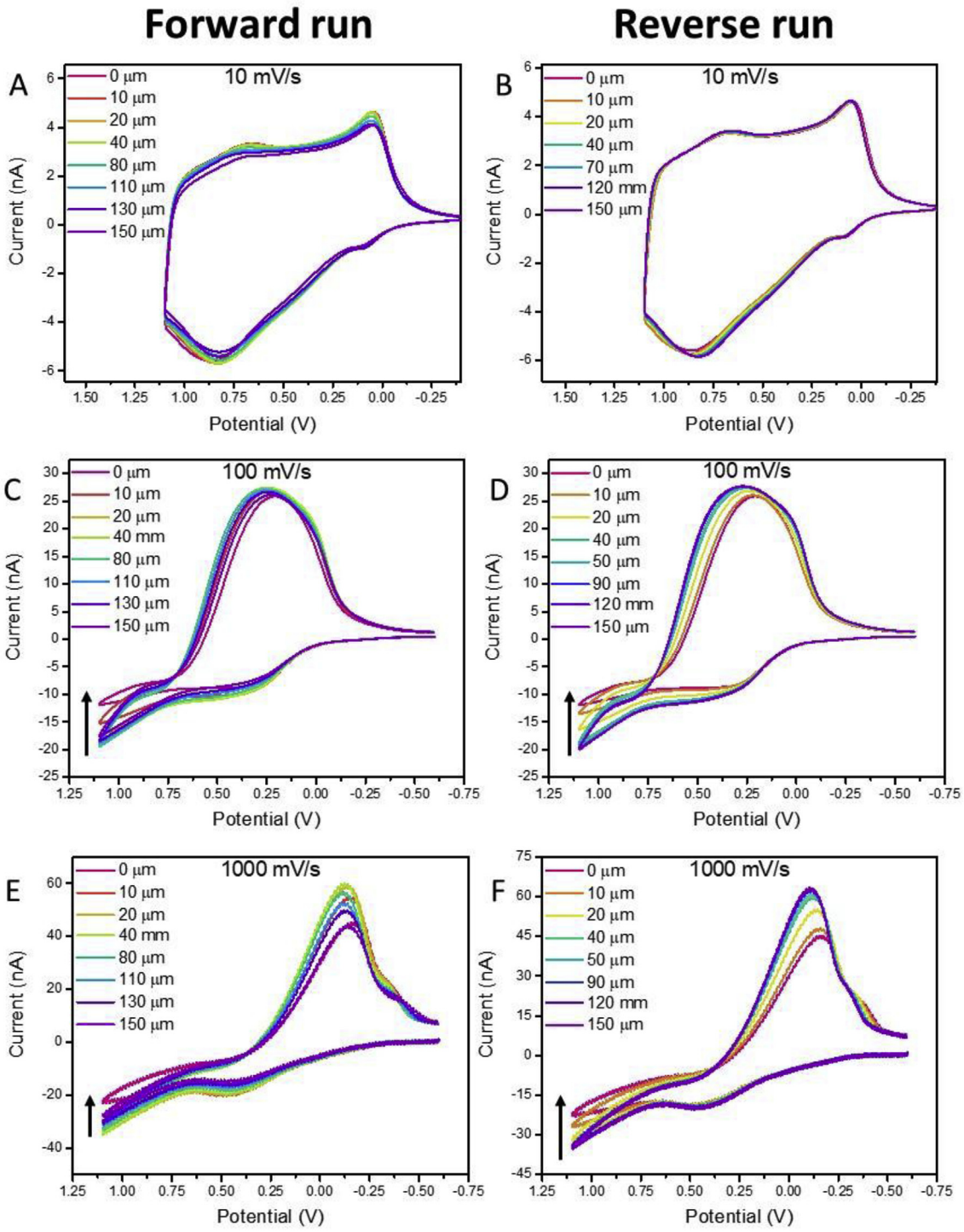

Fig. 8. Scan rate dependence of ion flux measurements at different distances from the surface for a r = 12.5 µm PEDOT well-probe UME. 1 mM $BARF^-$ in DMF vs Ag QRE. Arrows indicate the decrease in final current as the probe moves towards the surface. A, C and E) The probe is moved toward the point closest to the surface at 10, 100 and 1000 mV/s, respectively. B, D and F) Reverse run, the tip is moved from the surface toward infinite distance.

prevailed when a larger (25 µm-radius) well-probe was used (Figs. S9–12) but was lost when a smaller (r = 3.5 µm-radius) one was employed (Fig. S14).

While using smaller probes presents opportunities for improved lateral resolution, we also observed an inherent instability of the polymer well in such a small cavity over time (Fig. S14). Preconditioning of the well-probe in electrolyte showed decays in current over various cycles (Fig. S15A). The well-probe was also tested in electrolyte before and after use and showed overall decreased current in its CV profile indicative of film degradation or loss of material (Fig. S15B). Nevertheless, the two probes (r = 12.5 and 25 µm) that were successfully tested proved the viability of this technique to be used as the final current was fitted against experimental approach curves mediated by Fc (Fig. 5 and Fig. S10). Scan rates above 25 mV/s showed comparable results, with 100 mV/s showing the closest fit. At 10 mV/s, the curve strongly deviates from

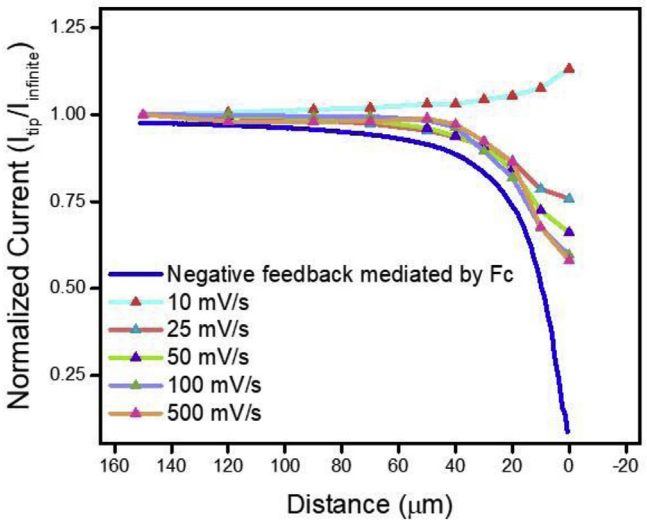

Fig. 9. Ion-responsive approach curves for a r = 12.5 μm PEDOT well-probe at different scan rates (see Fig. 8). Values for each point obtained from normalizing final charging current at different distances from the surface for the reverse run at 1 mM $BARF^-$ in DMF.

theory. Differences when trying to fit the theory to the CV-PAC at different scan rates can also be attributed to the fact that the phenomena associated with the charging and discharging of the probe are different than those considered for a normal conducting surface on which a faradaic process is responsible for the observed current. Therefore, modifications to the theory need to be made to better fit the chemistry of our probe. Nonetheless, the agreement with the general trend shows promise in the employment of large anions as electrolytes to measure ion flux with SECM.

4. Conclusions

We have presented the fabrication of conducting polymer well-probes and their application for redox and ionic measurements using SECM. We explored the use of CP-modified disks and CP-well probes. Under operating conditions, the well-probes showed a stable and reproducible response and comparable spatial resolution to conventional Pt probes. When using a mediator, feedback approach curves can be fit to negative feedback theory. CV-PAC SECM mode was explored for ionic flux processes using these well-probes but will require further optimization for fitting. A conductive substrate was successfully imaged both while biased and unbiased and compared well with images produced using a conventional Pt UME. Also, an unusual mediator like DMcT was successfully used to image topography on an insulating substrate thanks to the electrocatalytic effect PEDOT has on the molecule, further establishing the usefulness of these probes for species that foul conventional materials such as Pt used for SECM probes. This application demonstrates the versatility of the probe as it extends into enabling the use of organosulfur compounds as mediators. CP well-probes open opportunities in the study and characterization of processes involved in the characterization of energy materials, such as those found in ion-batteries and sulfur-containing electrolytes. Overall, this probe shows promise as a convenient and easy method to access and study systems that have traditionally been out of reach with normal metallic probes.

Declaration of interests

The authors declare that they have no known competing financial interests or personal relationships that could have appeared to influence the work reported in this paper.

Acknowledgements

This work was supported by the National Science Foundation under CHE 17-09391. Sample characterization was carried out in part in the Frederick Seitz Materials Research Laboratory Central Facilities, University of Illinois. M.A.C. would like to thank Jingshu Hui and Michael Counihan for help in the fabrication of substrates and Kenneth Hernandez-Burgos and Zachary Gossage for fruitful discussions.

Appendix A. Supplementary data

Supplementary data to this article can be found online at https://doi.org/10.1016/j.aca.2019.04.022.

References

[1] P. Schwager, H. Bülter, I. Plettenberg, G. Wittstock, Review of local in situ probing techniques for the interfaces of lithium-ion and lithium–oxygen batteries, Energy Technol. 4 (2016) 1472–1485, https://doi.org/10.1002/ente.201600141.
[2] Y. Takahashi, A. Kumatani, H. Munakata, H. Inomata, K. Ito, K. Ino, H. Shiku, P.R. Unwin, Y.E. Korchev, K. Kanamura, T. Matsue, Nanoscale visualization of redox activity at lithium-ion battery cathodes, Nat. Commun. 5 (2014) 5450, https://doi.org/10.1038/ncomms6450.
[3] R.M. Souto, L. Fernández-Mérida, S. González, SECM imaging of interfacial processes in defective organic coatings applied on metallic substrates using oxygen as redox mediator, Electroanalysis 21 (2009) 2640–2646, https://doi.org/10.1002/elan.200900232.
[4] Y. Zhu, D.E. Williams, Scanning electrochemical microscopic observation of a precursor state to pitting corrosion of stainless steel, J. Electrochem. Soc. 144 (1997) L43–L45, https://doi.org/10.1149/1.1837487.
[5] D. Polcari, P. Dauphin-Ducharme, J. Mauzeroll, Scanning electrochemical microscopy: a comprehensive review of experimental parameters from 1989 to 2015, Chem. Rev. 116 (2016) 13234–13278, https://doi.org/10.1021/acs.chemrev.6b00067.
[6] P. Sun, F.O. Laforge, M.V. Mirkin, Scanning electrochemical microscopy in the 21st century, Phys. Chem. Chem. Phys. 9 (2007) 802–823, https://doi.org/10.1039/B612259K.
[7] Y. Takahashi, A. Kumatani, H. Shiku, T. Matsue, Scanning probe microscopy for nanoscale electrochemical imaging, Anal. Chem. 89 (2017) 342–357, https://doi.org/10.1021/acs.analchem.6b04355.
[8] J.H. Bae, Y. Yu, M.V. Mirkin, Diffuse layer effect on electron-transfer kinetics measured by scanning electrochemical microscopy (SECM), J. Phys. Chem. Lett. 8 (2017) 1338–1342, https://doi.org/10.1021/acs.jpclett.7b00161.
[9] Y. Shao, M.V. Mirkin, Scanning electrochemical microscopy (SECM) of facilitated ion transfer at the Liquid|liquid Interface1Dedicated to professor K.B. Oldham on the occasion of his retirement from trent University.1, J. Electroanal. Chem. 439 (1997) 137–143, https://doi.org/10.1016/S0022-0728(97)00378-1.
[10] G. Wittstock, Modification and characterization of artificially patterned enzymatically active surfaces by scanning electrochemical microscopy, Fresenius J. Anal. Chem. 370 (2001) 303–315, https://doi.org/10.1007/s002160100795.
[11] S. Lhenry, Y.R. Leroux, P. Hapiot, Chemically irreversible redox mediator for SECM kinetics investigations: determination of the absolute tip-sample distance, Anal. Chem. 85 (2013) 1840–1845, https://doi.org/10.1021/ac303226e.
[12] S. Lhenry, B. Boichard, Y.R. Leroux, P. Even-Hernandez, V. Marchi, P. Hapiot, Photo-electrochemical properties of quantum rods studied by scanning electrochemical microscopy, Phys. Chem. Chem. Phys. 19 (2017) 4627–4635, https://doi.org/10.1039/C6CP07143K.
[13] F. Li, P.R. Unwin, Scanning electrochemical microscopy (SECM) of photoinduced electron transfer kinetics at liquid/liquid interfaces, J. Phys. Chem. C 119 (2015) 4031–4043, https://doi.org/10.1021/jp510333d.
[14] M. Nebel, T. Erichsen, W. Schuhmann, Constant-distance mode SECM as a tool to visualize local electrocatalytic activity of oxygen reduction catalysts, Beilstein J. Nanotechnol. 5 (2014) 141–151, https://doi.org/10.3762/bjnano.5.14.
[15] F.-R.F. Fan, B. Liu, J. Mauzeroll, 12 - scanning electrochemical microscopy, in: C.G. Zoski (Ed.), Handb. Electrochem, Elsevier, Amsterdam, 2007, pp. 471–540, https://doi.org/10.1016/B978-044451958-0.50025-2.
[16] M.A. Edwards, S. Martin, A.L. Whitworth, J.V. Macpherson, P.R. Unwin, Scanning electrochemical microscopy: principles and applications to biophysical systems, Physiol. Meas. 27 (2006) R63, https://doi.org/10.1088/0967-3334/27/12/R01.
[17] A.J. Bard, M.V. Mirkin, Chapter 16: scanning probe techniques, in: Scanning Electrochemical Microscopy, second ed., CRC Press, 2012, pp. 669–675.

[18] G. Gyetvai, L. Nagy, A. Ivaska, I. Hernádi, G. Nagy, Solid contact micropipette ion selective electrode II: potassium electrode for SECM and in vivo applications, Electroanalysis 21 (2009) 1970–1976, https://doi.org/10.1002/elan.200904617.
[19] G. Gyetvai, S. Sundblom, L. Nagy, A. Ivaska, G. Nagy, Solid contact micropipette ion selective electrode for potentiometric SECM, Electroanalysis 19 (2007) 1116–1122, https://doi.org/10.1002/elan.200703831.
[20] J. Kim, C. Renault, N. Nioradze, N. Arroyo-Currás, K.C. Leonard, A.J. Bard, Electrocatalytic activity of individual Pt nanoparticles studied by nanoscale scanning electrochemical microscopy, J. Am. Chem. Soc. 138 (2016) 8560–8568, https://doi.org/10.1021/jacs.6b03980.
[21] J. Velmurugan, J.-M. Noël, W. Nogala, M.V. Mirkin, Nucleation and growth of metal on nanoelectrodes, Chem. Sci. 3 (2012) 3307–3314, https://doi.org/10.1039/C2SC21005C.
[22] M.V. Mirkin, W. Nogala, J. Velmurugan, Y. Wang, Scanning electrochemical microscopy in the 21st century. Update 1: five years after, Phys. Chem. Chem. Phys. 13 (2011) 21196–21212, https://doi.org/10.1039/C1CP22376C.
[23] J.V. Macpherson, P.R. Unwin, Combined scanning electrochemical-atomic force microscopy, Anal. Chem. 72 (2000) 276–285.
[24] Y. Hirata, S. Yabuki, F. Mizutani, Application of integrated SECM ultra-microelectrode and AFM force probe to biosensor surfaces, Bioelectrochem. Amst Neth. 63 (2004) 217–224, https://doi.org/10.1016/j.bioelechem.2004.01.001.
[25] J. Velmurugan, A. Agrawal, S. An, E. Choudhary, V. Szalai, Fabrication of scanning electrochemical microscopy-atomic force microscopy (SECM-AFM) probes to image surface topography and reactivity at the nanoscale, Anal. Chem. 89 (2017) 2687–2691, https://doi.org/10.1021/acs.analchem.7b00210.
[26] P. Knittel, H. Zhang, C. Kranz, G.G. Wallace, M.J. Higgins, Probing the PEDOT: PSS/cell interface with conductive colloidal probe AFM-SECM, Nanoscale 8 (2016) 4475–4481, https://doi.org/10.1039/C5NR07155K.
[27] J. Wiedemair, J.-S. Moon, D.E. Eaton, B. Mizaikoff, C. Kranz, Combined AFM-SECM: towards a novel platform for imaging microbiosensors, in: O. Dössel, W.C. Schlegel (Eds.), World Congr. Med. Phys. Biomed. Eng. Sept. 7 - 12 2009 Munich Ger, Springer Berlin Heidelberg, 2010, pp. 372–375.
[28] A. Anne, E. Cambril, A. Chovin, C. Demaille, C. Goyer, Electrochemical atomic force microscopy using a tip-attached redox mediator for topographic and functional imaging of nanosystems, ACS Nano 3 (2009) 2927–2940, https://doi.org/10.1021/nn9009054.
[29] S.-X. Guo, P.R. Unwin, A.L. Whitworth, J. Zhang, Microelectrochemical Techniques for Probing Kinetics Adt Liquid/Liquid Interfaces, 2004, https://doi.org/10.3184/0079674044037441.
[30] M.L. Colombo, J.V. Sweedler, M. Shen, Nanopipet-based liquid–liquid interface probes for the electrochemical detection of acetylcholine, tryptamine, and serotonin via ionic transfer, Anal. Chem. 87 (2015) 5095–5100, https://doi.org/10.1021/ac504151e.
[31] Y. Shao, M.V. Mirkin, Probing ion transfer at the liquid/liquid interface by scanning electrochemical microscopy (SECM), J. Phys. Chem. B 102 (1998) 9915–9921, https://doi.org/10.1021/jp9828282.
[32] S. Amemiya, J. Kim, A. Izadyar, B. Kabagambe, M. Shen, R. Ishimatsu, Electrochemical sensing and imaging based on ion transfer at liquid/liquid interfaces, Electrochim. Acta 110 (2013), https://doi.org/10.1016/j.electacta.2013.03.098.
[33] Z.J. Barton, J. Rodríguez-López, Fabrication and demonstration of mercury disc-well probes for stripping-based cyclic voltammetry scanning electrochemical microscopy, Anal. Chem. 89 (2017) 2716–2723, https://doi.org/10.1021/acs.analchem.6b04022.
[34] Z.J. Barton, J. Rodríguez-López, Cyclic voltammetry probe approach curves with alkali amalgams at mercury sphere-cap scanning electrochemical microscopy probes, Anal. Chem. 89 (2017) 2708–2715, https://doi.org/10.1021/acs.analchem.6b04093.
[35] Z.J. Barton, J. Rodríguez-López, Emerging scanning probe approaches to the measurement of ionic reactivity at energy storage materials, Anal. Bioanal. Chem. 408 (2016) 2707–2715, https://doi.org/10.1007/s00216-016-9373-7.
[36] K. Hernández-Burgos, Z.J. Barton, J. Rodríguez-López, Finding harmony between ions and electrons: new tools and concepts for emerging energy storage materials, Chem. Mater. 29 (2017) 8918–8931, https://doi.org/10.1021/acs.chemmater.7b02243.
[37] J. Hui, Z.T. Gossage, D. Sarbapalli, K. Hernández-Burgos, J. Rodríguez-López, Advanced electrochemical analysis for energy storage interfaces, Anal. Chem. 91 (2019) 60–83, https://doi.org/10.1021/acs.analchem.8b05115.
[38] G.A. Edwards, A.J. Bergren, M.D. Porter, 8 - chemically modified electrodes, in: C.G. Zoski (Ed.), Handb. Electrochem, Elsevier, Amsterdam, 2007, pp. 295–327, https://doi.org/10.1016/B978-044451958-0.50021-5.
[39] M.E.G. Lyons, Charge percolation in electroactive polymers, in: Electroact. Polym. Electrochem, Springer, Boston, MA, 1994, pp. 1–235, https://doi.org/10.1007/978-1-4757-5070-6_1.
[40] D.P. Manica, Y. Mitsumori, A.G. Ewing, Characterization of electrode fouling and surface regeneration for a platinum electrode on an electrophoresis microchip, Anal. Chem. 75 (2003) 4572–4577, https://doi.org/10.1021/ac034235f.
[41] W. Lu, G.G. Wallace, M.D. Imisides, Development of conducting polymer modified electrodes for the detection of phenol, Electroanalysis 14 (2002) 325–332, https://doi.org/10.1002/1521-4109(200203)14:5<325::AID-ELAN325>3.0.CO;2-9.
[42] J. Heinze, B.A. Frontana-Uribe, S. Ludwigs, Electrochemistry of conducting polymers—persistent models and new concepts, Chem. Rev. 110 (2010) 4724–4771, https://doi.org/10.1021/cr900226k.
[43] D.N. Nguyen, H. Yoon, Recent advances in nanostructured conducting polymers: from synthesis to practical applications, Polymers 8 (2016) 118, https://doi.org/10.3390/polym8040118.
[44] J.G. Ibanez, M.E. Rincón, S. Gutierrez-Granados, M. Chahma, O.A. Jaramillo-Quintero, B.A. Frontana-Uribe, Conducting polymers in the fields of energy, environmental remediation, and chemical–chiral sensors, Chem. Rev. (2018), https://doi.org/10.1021/acs.chemrev.7b00482.
[45] Y. Xia, K. Sun, J. Ouyang, Solution-processed metallic conducting polymer films as transparent electrode of optoelectronic devices, Adv. Mater. 24 (2012) 2436–2440, https://doi.org/10.1002/adma.201104795.
[46] K. Kłucińska, E. Jaworska, P. Gryczan, K. Maksymiuk, A. Michalska, Synthesis of conducting polymer nanospheres of high electrochemical activity, Chem. Commun. 51 (2015) 12645–12648, https://doi.org/10.1039/C5CC03705K.
[47] Y. Kiya, G.R. Hutchison, J.C. Henderson, T. Sarukawa, O. Hatozaki, N. Oyama, H.D. Abruña, Elucidation of the redox behavior of 2,5-Dimercapto-1,3,4-thiadiazole (DMcT) at poly(3,4-ethylenedioxythiophene) (PEDOT)-Modified electrodes and application of the DMcT–PEDOT composite cathodes to lithium/lithium ion batteries, Langmuir 22 (2006) 10554–10563, https://doi.org/10.1021/la061213q.
[48] Y. Kiya, O. Hatozaki, N. Oyama, H.D. Abruña, Kinetic studies for the electrocatalytic reduction of bis(2-mercapto-1,3,4-thiadiazoyl)-5,5'-disulfide at a poly(3,4-ethylenedioxythiophene) film-modified electrode via rotating-disk electrode voltammetry, J. Phys. Chem. C 111 (2007) 13129–13136, https://doi.org/10.1021/jp073486f.
[49] A.R. Hillman, S.J. Daisley, S. Bruckenstein, Ion and solvent transfers and trapping phenomena during n-doping of PEDOT films, Electrochim. Acta 53 (2008) 3763–3771, https://doi.org/10.1016/j.electacta.2007.10.062.
[50] G. Inzelt, Conducting Polymers: A New Era in Electrochemistry, second ed., Springer-Verlag, Berlin Heidelberg, 2012. www.springer.com/us/book/9783642276200. (Accessed 2 July 2018).
[51] V. Venugopal, V. Venkatesh, R.G. Northcutt, J. Maddox, V.B. Sundaresan, Nanoscale polypyrrole sensors for near-field electrochemical measurements, Sensor. Actuator. B Chem. 242 (2017) 1193–1200, https://doi.org/10.1016/j.snb.2016.09.121.
[52] J. Wang, C. Wu, P. Wu, X. Li, M. Zhang, J. Zhu, Polypyrrole capacitance characteristics with different doping ions and thicknesses, Phys. Chem. Chem. Phys. (2017), https://doi.org/10.1039/C7CP02707A.
[53] X. Wang, B. Shapiro, E. Smela, Visualizing ion currents in conjugated polymers, Adv. Mater. 16 (2004) 1605–1609, https://doi.org/10.1002/adma.200400188.
[54] X. Wang, B. Shapiro, E. Smela, Modeling Charge Transport in Conjugated Polymers, Proc. SPIE 6168, Smart Structures and Materials 2006: Electroactive Polymer Actuators and Devices (EAPAD), 61680U (15 March 2006), 2006, https://doi.org/10.1117/12.655751.
[55] M.A. Rahman, M.-S. Won, Y.-B. Shim, Characterization of an EDTA bonded conducting polymer modified Electrode: its application for the simultaneous determination of heavy metal ions, Anal. Chem. 75 (2003) 1123–1129, https://doi.org/10.1021/ac0262917.
[56] M. Puida, A. Malinauskas, F. Ivanauskas, Modeling of electrocatalysis at conducting polymer modified electrodes: nonlinear current-concentration profiles, J. Math. Chem. 49 (2011) 1151–1162, https://doi.org/10.1007/s10910-011-9802-y.
[57] S. Kakhki, M.M. Barsan, E. Shams, C.M.A. Brett, New redox and conducting polymer modified electrodes for cholesterol biosensing, Anal. Methods. 5 (2013) 1199–1204, https://doi.org/10.1039/C3AY26409B.
[58] R.P. Singh, Prospects of organic conducting polymer modified electrodes: enzymosensors, Int. J. Electrochem. 2012 (2012) 14, https://doi.org/10.1155/2012/502707. Article ID 502707.
[59] H.-S. Wang, T.-H. Li, W.-L. Jia, H.-Y. Xu, Highly selective and sensitive determination of dopamine using a Nafion/carbon nanotubes coated poly(3-methylthiophene) modified electrode, Biosens. Bioelectron. 22 (2006) 664–669, https://doi.org/10.1016/j.bios.2006.02.007.
[60] E. Salamifar, M.A. Mehrgardi, M.F. Mousavi, Ion transport and degradation studies of a polyaniline-modified electrode using SECM, Electrochim. Acta 54 (2009) 4638–4646, https://doi.org/10.1016/j.electacta.2009.03.069.
[61] K. Borgwarth, N. Rohde, C. Ricken, M.L. Hallensleben, D. Mandler, J. Heinze, Electroless deposition of conducting polymers using the scanning electrochemical microscope, Adv. Mater. 11 (1999) 1221–1226, https://doi.org/10.1002/(SICI)1521-4095(199910)11:14<1221::AID-ADMA1221>3.0.CO;2-J.
[62] C. Kranz, G. Wittstock, H. Wohlschläger, W. Schuhmann, Imaging of microstructured biochemically active surfaces by means of scanning electrochemical microscopy, Electrochim. Acta 42 (1997) 3105–3111, https://doi.org/10.1016/S0013-4686(97)00158-8.
[63] E. Poverenov, M. Li, A. Bitler, M. Bendikov, Major effect of electropolymerization solvent on morphology and electrochromic properties of PEDOT films, Chem. Mater. 22 (2010) 4019–4025, https://doi.org/10.1021/cm100561d.
[64] G.G. Rodríguez-Calero, M.A. Lowe, Y. Kiya, H.D. Abruña, Electrochemical and computational studies on the electrocatalytic effect of conducting polymers toward the redox reactions of thiadiazole-based thiolate compounds, J. Phys. Chem. C 114 (2010) 6169–6176, https://doi.org/10.1021/jp9076504.
[65] A.G. Güell, I. Díez-Pérez, P. Gorostiza, F. Sanz, Preparation of reliable probes for electrochemical tunneling spectroscopy, Anal. Chem. 76 (2004) 5218–5222, https://doi.org/10.1021/ac035150h.

[66] J.E. Baur, R.M. Wightman, Diffusion coefficients determined with microelectrodes, J. Electroanal. Chem. Interfacial Electrochem. 305 (1991) 73–81, https://doi.org/10.1016/0022-0728(91)85203-2.
[67] Pandey, Handbook of Semiconductor Electrodeposition, CRC Press, 1996.
[68] M.V. Mirkin, T.C. Richards, A.J. Bard, Scanning electrochemical microscopy. 20. Steady-state measurements of the fast heterogeneous kinetics in the ferrocene/acetonitrile system, J. Phys. Chem. 97 (1993) 7672–7677, https://doi.org/10.1021/j100131a042.
[69] N. Oyama, T. Tatsuma, T. Sotomura, Organosulfur polymer batteries with high energy density, J. Power Sources 68 (1997) 135–138, https://doi.org/10.1016/S0378-7753(96)02586-4.
[70] R.A. Davoglio, S.R. Biaggio, R.C. Rocha-Filho, N. Bocchi, Bilayered nanofilm of polypyrrole and poly(DMcT) for high-performance battery cathodes, J. Power Sources 195 (2010) 2924–2927, https://doi.org/10.1016/j.jpowsour.2009.11.014.